

Efficient Construction and Simplification of Delaunay Meshes

(Supplementary Material)

Yong-Jin Liu
Tsinghua University

Chun-Xu Xu
Tsinghua University

Dian Fan
Tsinghua University

Ying He
Nanyang Technological University

1 Meshes with Boundaries

Sections 4 and 5 of the main text deal with construction and simplification of closed Delaunay meshes. Now we show that these algorithms can be easily extended to meshes with boundaries.

Let \widetilde{M} be an open manifold triangle mesh and $\partial\widetilde{M}$ its boundaries. We generalize the 1-ring neighborhood (cf. Definition 3 in the paper) to points on the boundary:

- If p is a boundary vertex $p \in \partial\widetilde{M}$, $N_1(p)$ consists of the triangles incident to p .
- If p lies on a boundary edge $e \in \partial\widetilde{M}$, $N_1(p)$ is the triangle containing e .

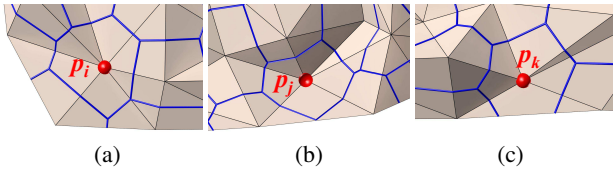


Figure 1: Delaunay mesh condition C2 for meshes with boundary. (a) A general case: the angles subtended by the boundary edges are acute, so the Voronoi cell $C(p_i)$ does not intersect any boundary edges at all. (b) A degenerate case: the angle subtended by the boundary edge is 90° , so the Voronoi cell $C(p_j)$ touches the edge at a single point. (c) A case of non-Delaunay mesh: the angle subtended by the boundary edge is obtuse, so condition C2 does not hold on vertex p_k .

We then present the sufficient condition for open Delaunay meshes.

Theorem 4 (Delaunay Mesh Condition for Open Meshes) Given a set P of points on an open mesh \widetilde{M} , if the geodesic Voronoi diagram $GVD(P)$ satisfies the following conditions,

- C1. for every point $p \in P$, the Voronoi cell $C(p)$ is contained in $N_1(p) \setminus \partial N_1(p)$;
- C2. for every interior point p , $(C(p) \cap \partial\widetilde{M})^o = \emptyset$, where X^o denotes the interior of X .

then its dual graph of $GVD(P)$ is a Delaunay mesh. The second condition C2 requires that each angle subtended by a boundary edge is less than or equal to $\frac{\pi}{2}$. See Figure 1. The existence theorem for open meshes has also a similar form of the closed meshes.

Theorem 5 (Existence of DM for Meshes With Boundary) If the point set S defined on an open mesh $\widetilde{M} = (\widetilde{V}, \widetilde{E}, \widetilde{F})$ satisfies the Delaunay mesh sampling criterion, then the geodesic Voronoi diagram $GVD(\widetilde{V} \cup S)$ satisfies conditions C1 and C2, hereby its dual graph $IDT(\widetilde{V} \cup S)$ is a DM.

We omit the proofs of Theorems 4 and 5, since they are similar to the counterpart of closed meshes. A boundary edge $e \in \partial\widetilde{M}$ is NLD if its subtended angle is greater than $\pi/2$. With a slight

modification, we can define the intervals on a boundary NLD edge (see Figure 2). Therefore, the NLD edge refinement algorithm (Algorithm 2 in the paper) can be trivially extended to open triangle meshes.

Algorithm 3 in the paper can also be modified to simplify open Delaunay meshes while preserving the boundaries. To define type-I and II removable vertices on boundaries, we require that the subtended angle by each boundary edge is acute (i.e., the C2 condition). Also, a boundary edge is always non-flippable. Following the original QEM method, we generate a perpendicular plane running through each boundary edge. These constraint planes are then converted into quadrics, weighted by a large penalty factor, and added into the initial quadrics for the endpoints of the edge.

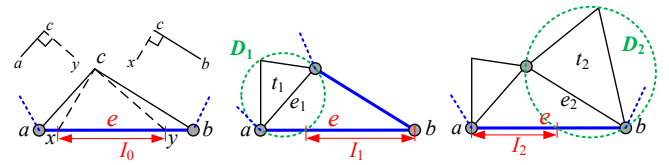
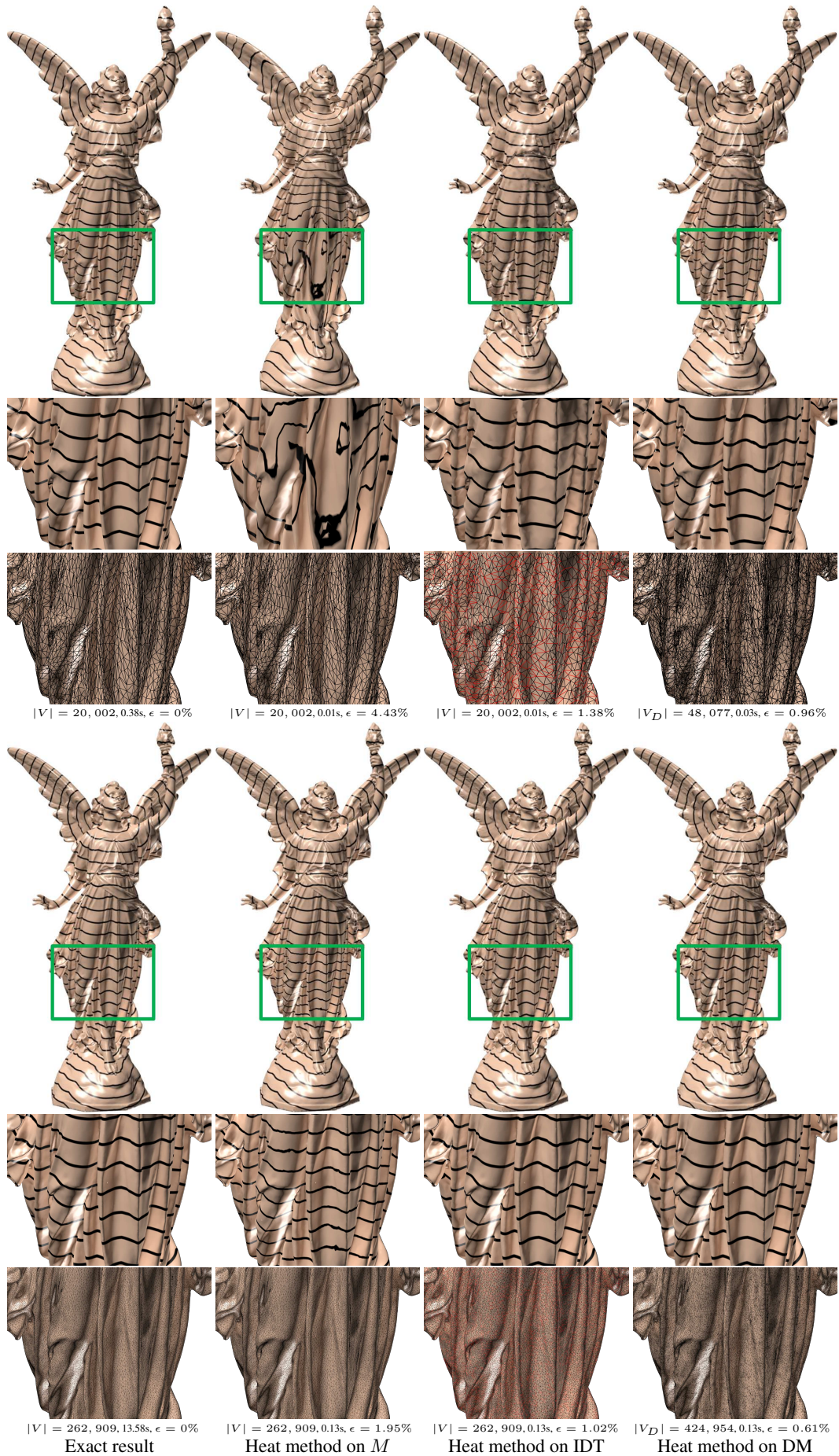


Figure 2: Consider a boundary NLD edge $e = (a, b)$. Left: define the interval $I_0 = [x, y]$, where $cx \perp cb$ and $cy \perp ca$. Middle: we consider intervals I_0 and I_1 when $\triangle abc$ has two boundary edges (in blue). Right: we consider three intervals I_0 , I_1 and I_2 when e is the only boundary edge of $\triangle abc$. Compare with Figure 6 in the paper.

2 Additional Experimental Results

This section presents additional results on DM construction, simplification and applications.



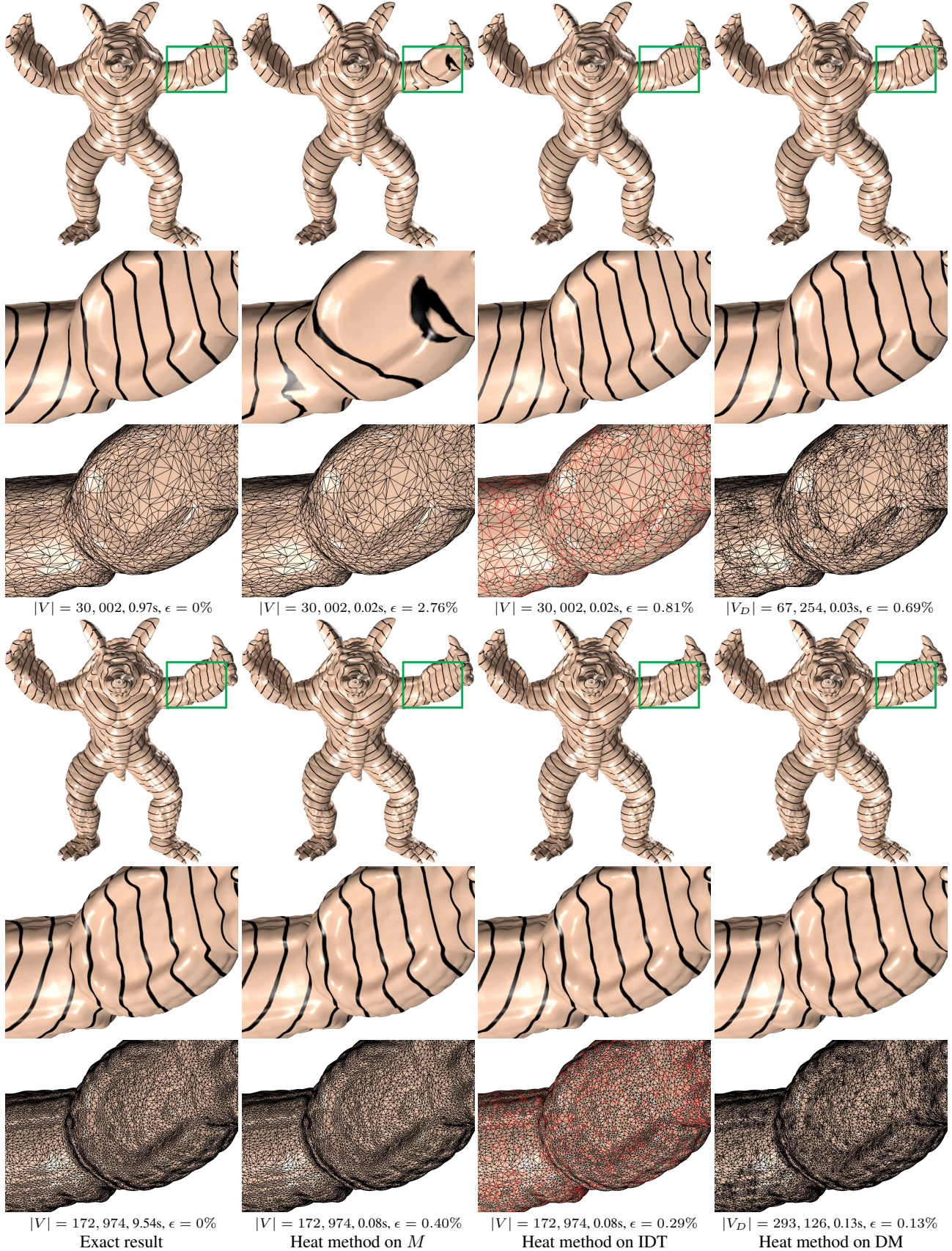


Figure 3: Computing geodesic distances using the heat method. Since the heat method solves a pair of elliptic linear systems, its accuracy highly depends on the mesh's Delaunay quality. DM can improve the accuracy of the heat method significantly. Since there are more vertices in DM than IDT, it takes the heat method slightly longer time on DM. The red edges in the IDT are geodesic paths (i.e., polylines).

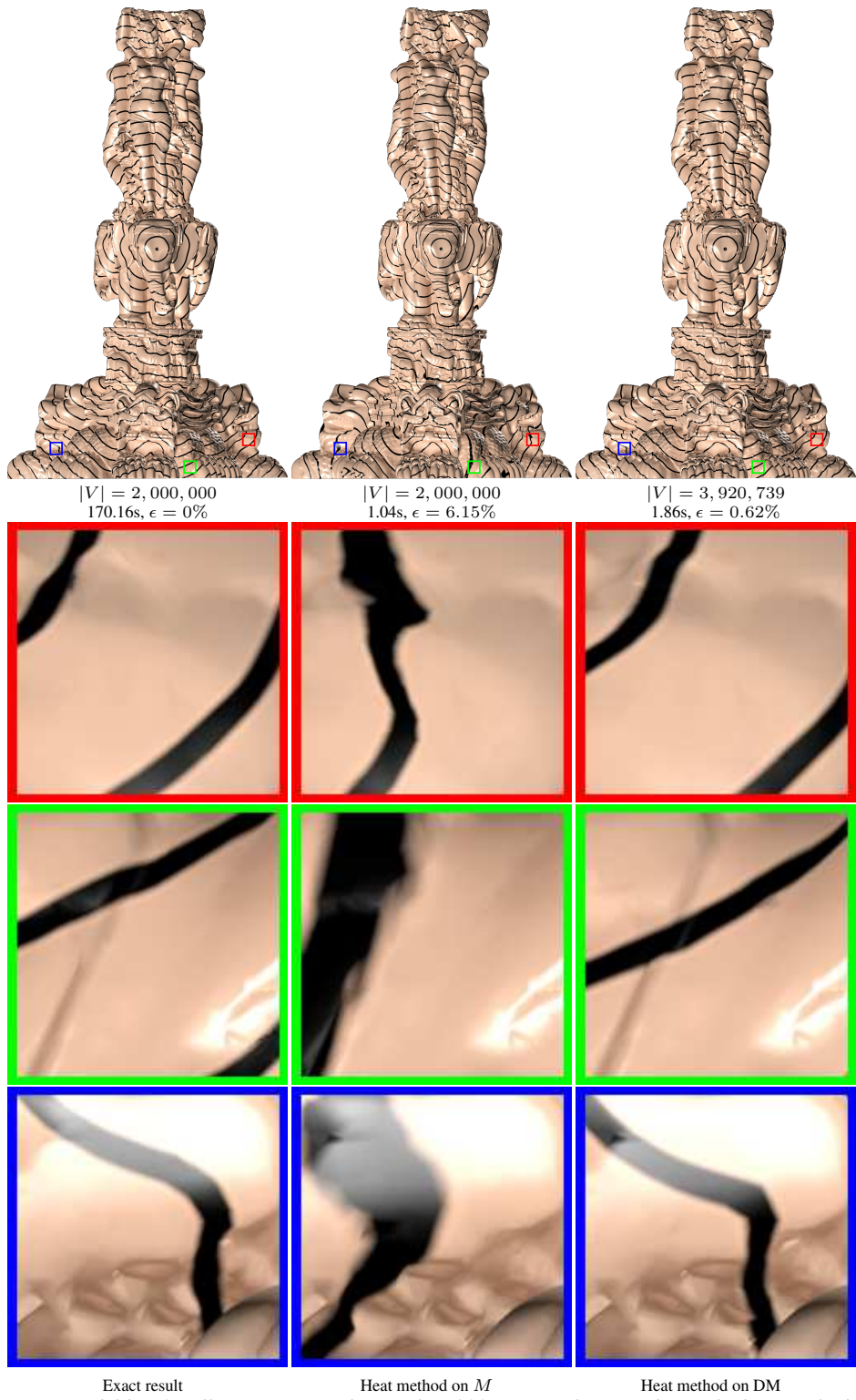


Figure 4: The Thai Statue model has 2 million vertices and more than 800K non-Delaunay edges. The heat method produces poor results on the original mesh with mean error 6.15%. Using the Delaunay mesh, the error drops to 0.62%.

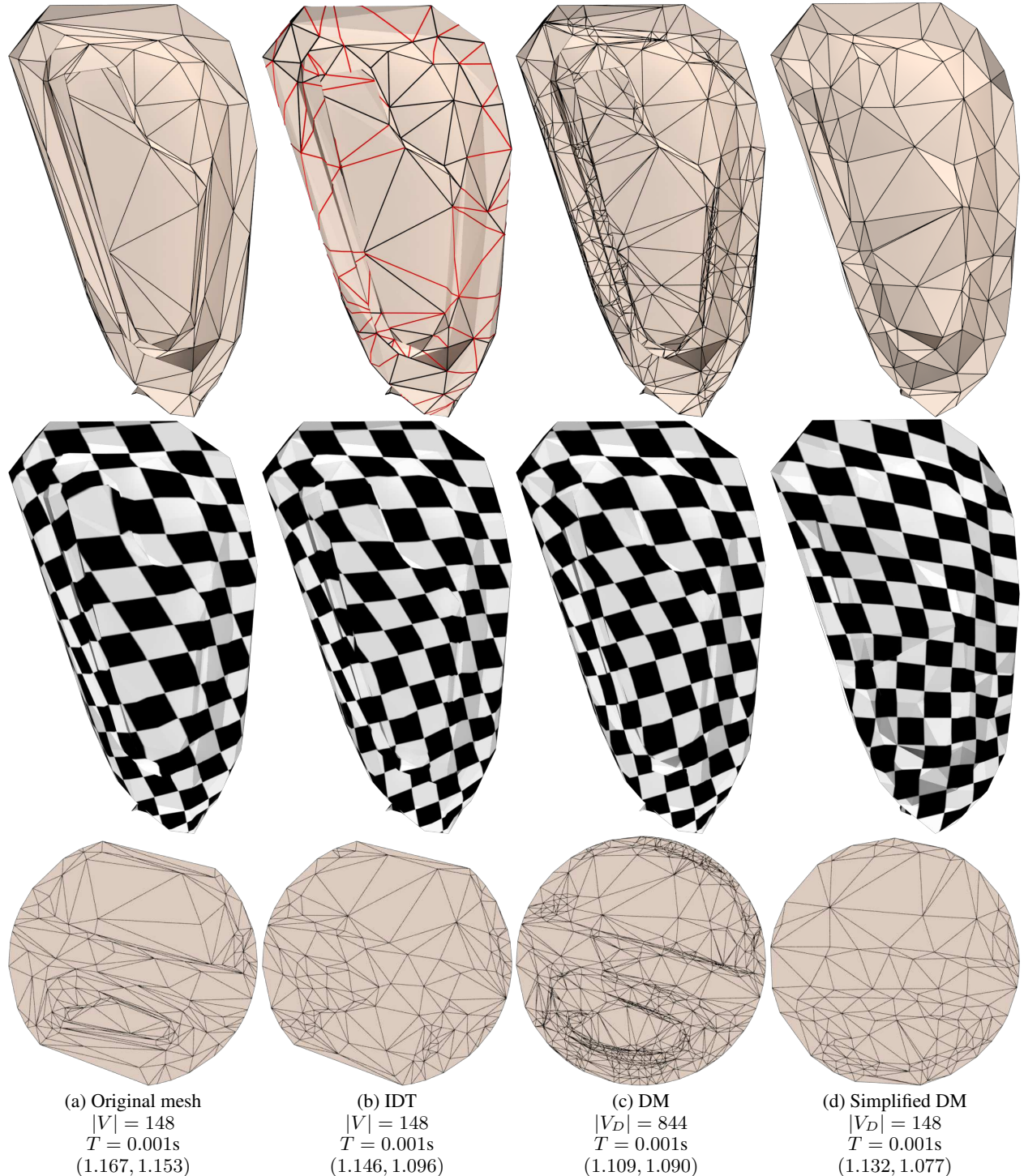


Figure 5: Parameterizing the Club model using the harmonic map. The boundary is mapped to a unit disk using arc-length parameterization. The tuple shows the angle distortion and area distortion, respectively. The DM-induced parameterization has the least angle distortion, whereas the simplified DM (with the same number of vertices as the input mesh) leads to result with the least area distortion.

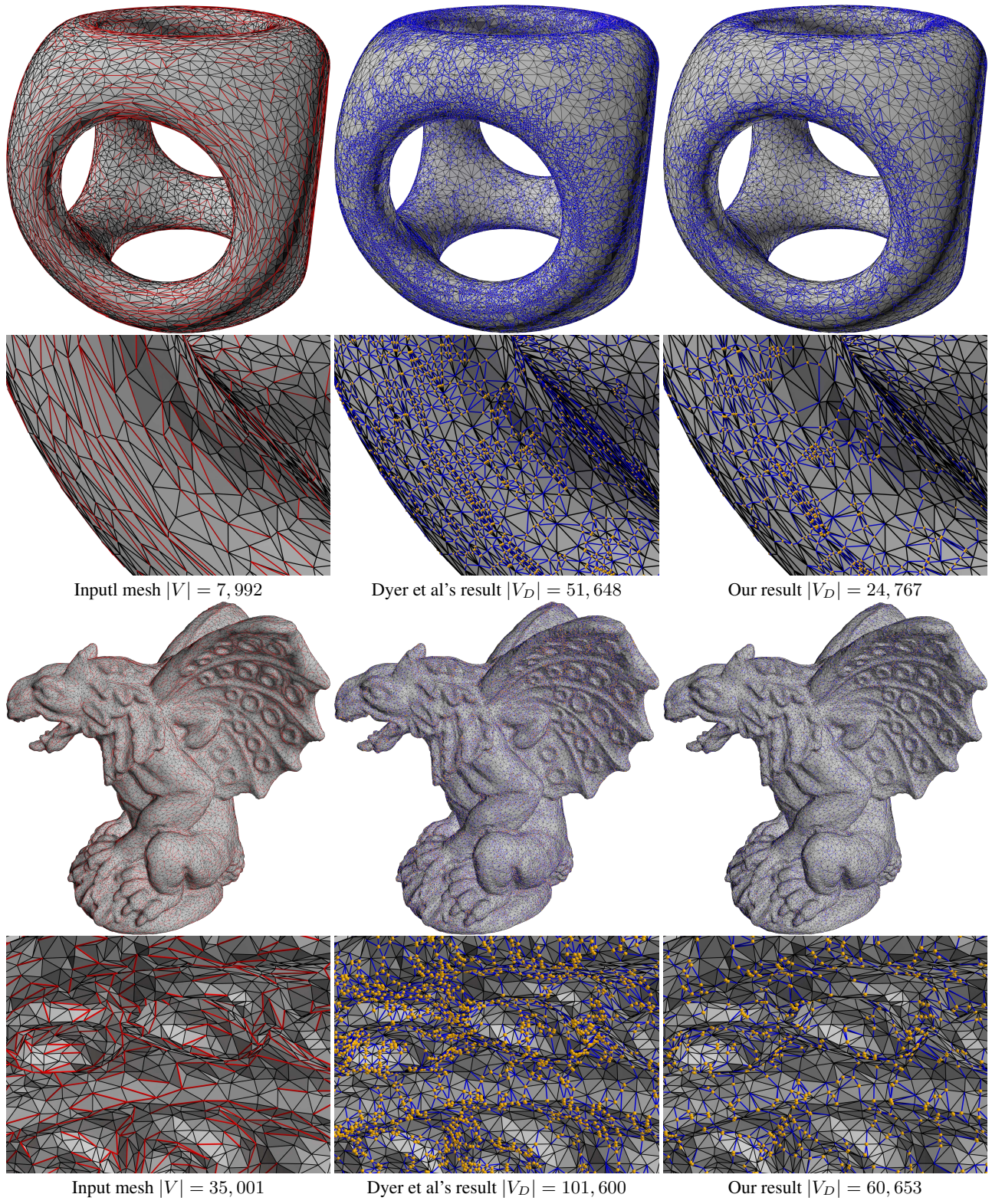


Figure 6: Our method produces the DM with significantly fewer vertices than Dyer et al.’s method. The added auxiliary points are in orange, the non-Delaunay edges in red and the added edges in blue.

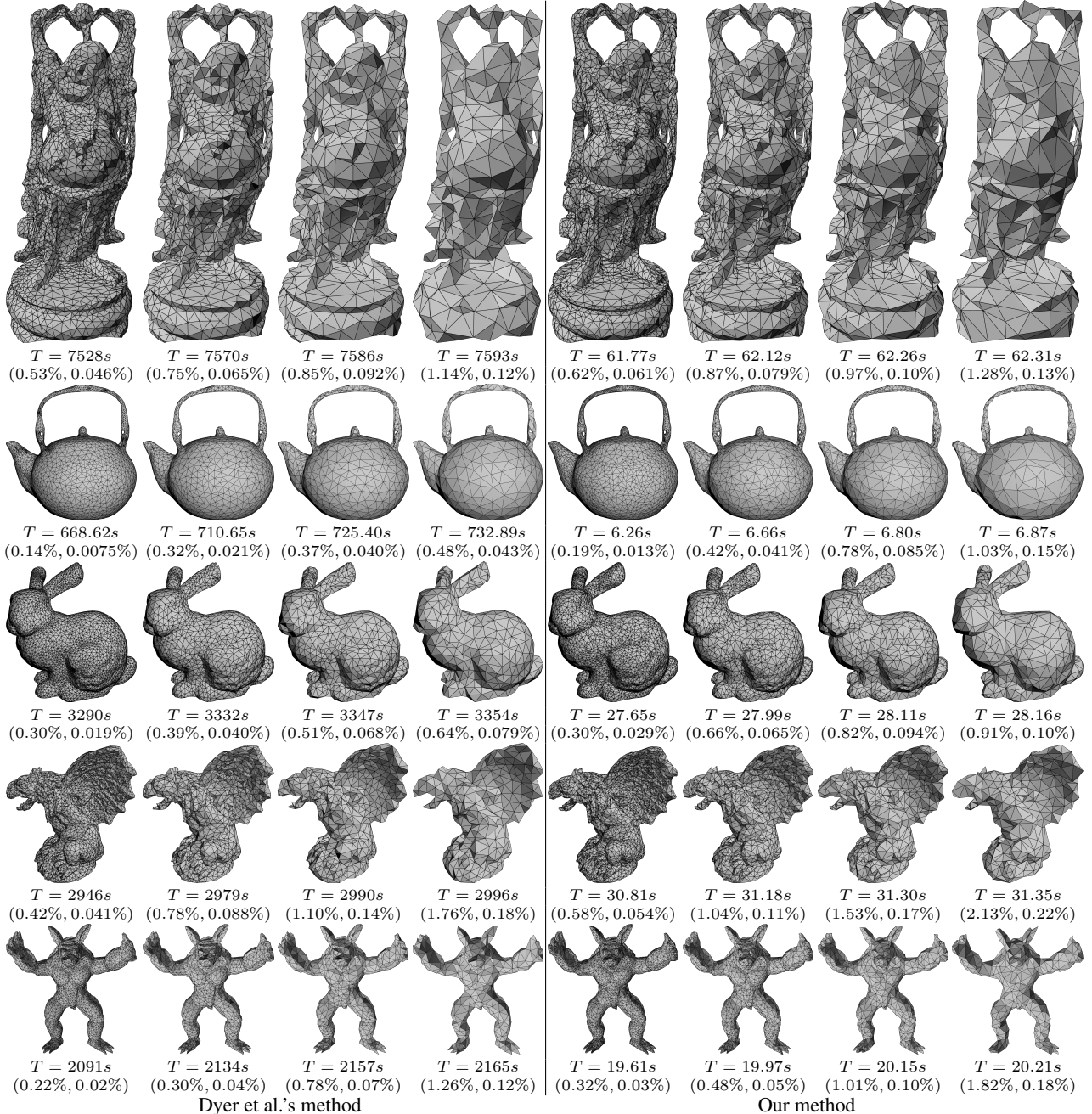


Figure 7: Comparison with Dyer et al.’s DM simplification algorithm. T is the running time and the tuple shows the maximal error ε_{\max} and the mean error $\varepsilon_{\text{mean}}$, respectively. The simplified DMs have 5K, 2K, 1K and 500 faces, respectively. Our method maintains a comparable level of accuracy of Dyer’s method, but runs two orders of magnitude faster than theirs.

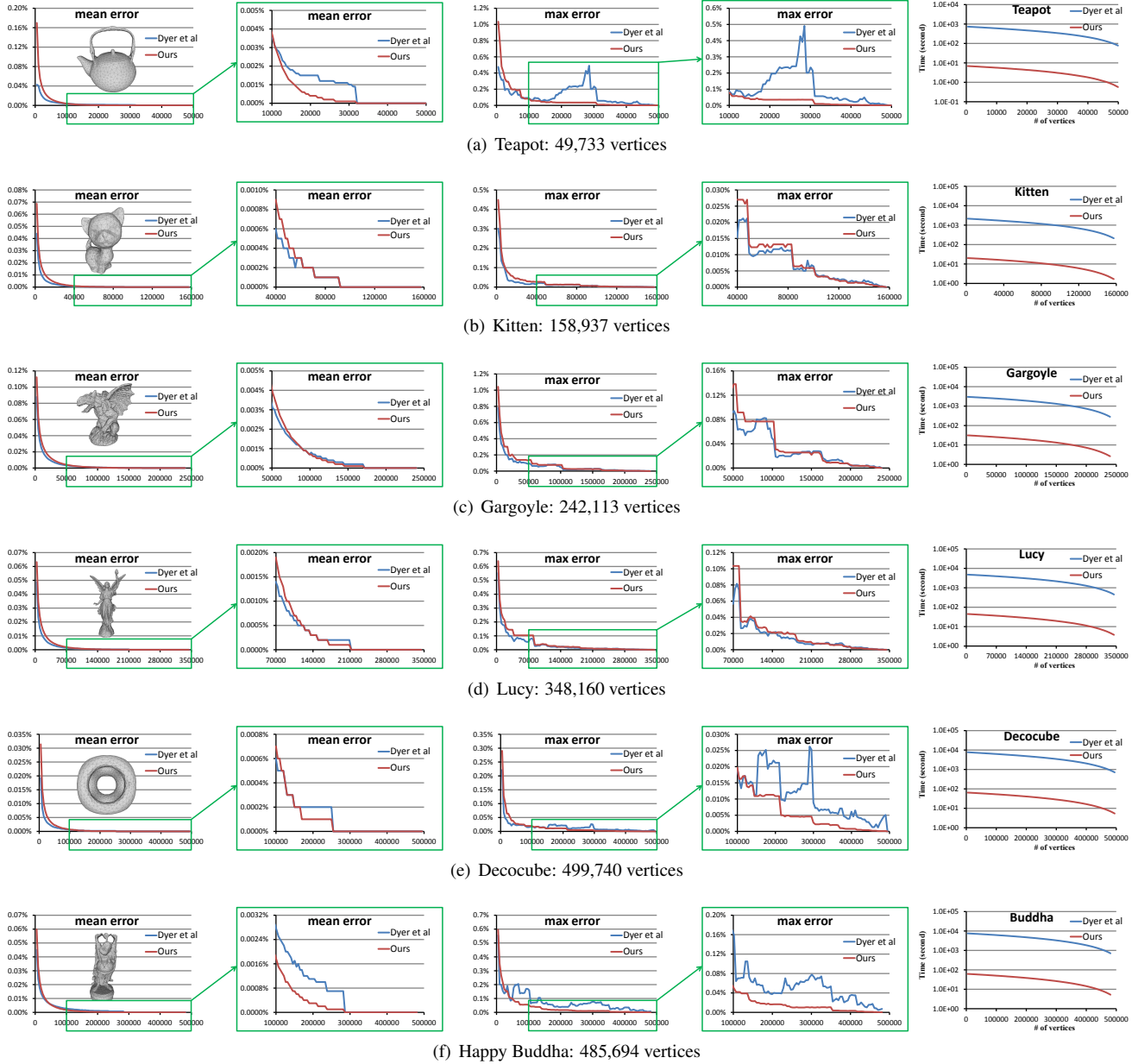


Figure 8: Delaunay mesh simplification. The models are scaled to a unit cube and the maximum error and mean error are measured by the Metro tool. The vertical axis in the last column shows the logarithm of time. Our method runs two orders of magnitude faster than Dyer et al's method, while producing results of comparable quality.